



Fermi National Accelerator Laboratory

FERMILAB-Pub-92/216-E

A Novel Electromagnetic Shower Maximum Position Detector

G. Apollinari, N.D. Giokaris, K. Goulianos, A. Titov, Z. Wu

The Rockefeller University

E. Hayashi, T. Kaneko, S. Kim, K. Kondo, S. Miyashita, H. Nakada, K. Takikawa, K. Yasuoka

University of Tsukuba

T. Kamon

Texas A&M University

V. Barnes

Purdue University

August 1992

Submitted to *Nuclear Instruments and Methods A*

Disclaimer

This report was prepared as an account of work sponsored by an agency of the United States Government. Neither the United States Government nor any agency thereof, nor any of their employees, makes any warranty, express or implied, or assumes any legal liability or responsibility for the accuracy, completeness, or usefulness of any information, apparatus, product, or process disclosed, or represents that its use would not infringe privately owned rights. Reference herein to any specific commercial product, process, or service by trade name, trademark, manufacturer, or otherwise, does not necessarily constitute or imply its endorsement, recommendation, or favoring by the United States Government or any agency thereof. The views and opinions of authors expressed herein do not necessarily state or reflect those of the United States Government or any agency thereof.

A Novel Electromagnetic Shower Maximum Position Detector

G. Apollinari, N. D. Giokaris, K. Goulianos, A. Titov, Z. Wu
The Rockefeller University

E. Hayashi, T. Kaneko, S. Kim, K. Kondo, S. Miyashita, H. Nakada, K. Takikawa, K. Yasuoka
University of Tsukuba

T. Kamon
Texas A&M University

V. Barnes
Purdue University

July 15, 1992

(Submitted to Nuclear Instruments and Methods A)

Abstract

We present test-beam results of a position-sensitive electromagnetic shower-maximum detector consisting of 1 cm wide scintillator strips read out with wave length shifting fibers. The detector is unique in that the strips are defined by deep "isolation" grooves carved in a single slab of scintillator. This novel design facilitates construction and results in reproducibly uniform detector elements. Operated at a depth of six radiation lengths inside an electromagnetic calorimeter, the detector yielded a position resolution of ± 1.5 mm for 100 GeV electrons

1. Introduction

We report results on the spacial resolution obtained with a circular position-sensitive Shower Maximum Detector (SMD) operated at a depth of six radiation lengths inside an electromagnetic (EM) calorimeter exposed to high energy electrons in a test beam at Fermilab. Consisting basically of 1 cm wide scintillator strips read out with wavelength shifting (WLS) fibers, the SMD was constructed from a single slab of scintillator, in which the strips were defined by deep grooves filled with highly reflective aluminum "separators". This novel design was originally chosen to facilitate the construction of a required circular detector. However, since it results in reproducibly uniform detector elements, it has become a leading candidate for the SMD's of large collider projects, such as the CDF (Collider Detector at Fermilab) plug upgrade and the SDC (Solenoidal Detector Collaboration) calorimeter.

The detector described here was built in conjunction with two small electromagnetic tile-fiber calorimeters intended to cover the region between the beam pipe and the forward EM calorimeters of CDF [1]. As their function would be to "plug" the small two-degree holes in the forward region, these calorimeters were dubbed the "Microplugs". In order to fit tightly inside the octagonal holes of the CDF forward EM calorimeters, the microplugs were made of trapezoidal towers, as shown in Fig. 1. For easy installation around the beam pipe (without disassembling the pipe), each microplug was made of two four-tower sections. Such a "one-half microplug" section, including a shower maximum position detector, was exposed to a test beam at Fermilab in December 1991. In what follows, we describe the design and construction of the microplug and its SMD, and present results on position resolution and lateral shower profiles obtained with the SMD. For completeness, and because of their relevance to the SMD results, we also present results on energy resolution, linearity and shower longitudinal profiles of the microplug calorimeter for electron energies from 10 to 150 GeV.

2. Detector design and construction

Each microplug tower consists of twelve 1 cm thick lead plates and thirteen 6 mm thick SCSN81 scintillator tiles viewed by 1 mm diameter BCF91A wavelength shifting fibers. The trapezoid-shaped tiles were polished on all sides and were "boxed" in aluminum covers made of "specular" 0.012 inch thick aluminum sheet of 86% reflectivity. No glue was used to keep the fibers in the tile grooves. The fibers were simply pushed into the grooves through small slots on the aluminum covers.

The shower-maximum position detector was also made of 6 mm thick SCSN81 scintillator, as shown in Fig. 2. An 11" diameter piece of scintillator with a 4.5" hole at its center was partially

separated into 8 circular strips by 4.5 mm deep grooves of 1.1 mm width. In the center of each 13/32" (10.3 mm) wide strip a 1.1 mm wide by 1.2 mm deep groove was milled to accept the read-out fiber. The circular piece was then cut into two halves along the horizontal thick line shown in the figure. A groove 10 mm wide and 1.2 mm deep was milled along the vertical line as shown to facilitate fiber insertion into the right and left quadrants of the detector. Reflective aluminum strips 4.5 mm wide by 0.012 inch thick were inserted in the deep grooves for (partial) optical isolation of the scintillator strips. The scintillator was then boxed in 0.5 mm thick reflective aluminum covers as shown in Fig. 3 and the fibers were pushed into their grooves through slots on the front cover (the back cover had no slots). The 3/32" diameter holes shown are for allowing passage of stainless steel tubes that run through the length of the calorimeter and are used to guide a radioactive wire past the tiles of each tower for calibration.

Fig. 4 shows the tower layout of the one-half microplug test module. The fibers from towers 2, 3 and 4 are viewed by Hamamatsu R4125 18 mm dia. photo-multiplier tubes (PMT's). Tower 1 is viewed by a 2 inch dia. RCA-8575 PMT through one end of the fiber of each tile, while the other end goes to a Hamamatsu H4140 Multi-Channel PMT for recording the pulse height of each individual tile so as to obtain the longitudinal shower profile. The MCPMT is also used to record the pulse height of the SMD, of which there are 16 channels (8 in each quadrant). A schematic drawing of the fiber arrangement is shown in Fig. 5. The 2 inch PMT views the fibers from tower 1 through a lucite light-mixer. The same light-mixer is used to provide uniform illumination of the fibers by a green LED mounted at the end of the mixer near the PMT photocathode. The LED is used to cross-calibrate the MCPMT pixels and all other PMT's, as shown. The calibration is fixed by an additional PMT, not shown in the figure, which views an Americium-241 alpha source in addition to the LED.

The MCPMT is coupled to the microplug fibers through a fiber cable with optical connectors on each side. The connector on the microplug side handles a total of 45 fibers: 13 from tower 1, 16 from the SMD strips and 16 from the LED for cross-calibrating the SMD pixels of the MCPMT. The connector on the MCPMT handles 29 fiber channels, as the 16 calibration fibers double-up with the SMD fibers and each pair is guided onto a single pixel of the tube. This connector has a total of 36 channels, which is the result of "wiring-up" every third channel of the 256-channel MCPMT to obtain a 6x6 matrix. This was done in order to reduce the electronic cross-talk between neighboring channels, which would normally be about 50%, down to a level of about 10%.

3. Source and LED calibrations

As mentioned previously, provision was made for calibration of all tiles with a Cs-137 (gamma) source in the usual CDF manner: the source was mounted at the tip of a wire which could be pushed past each tile guided through 0.080 inch diameter stainless steel "source tubes". A total of 11 source tubes were used in the one-half microplug module, as shown in Fig. 4, so that each tile could be tested at three different locations.

A special low gear to the source reel permitted accurate measurement of phototube DC current as the source passed by each tile of a tower. The results of this measurement show that the response of the 52 tiles of the 4 towers is uniform to within about $\pm 5\%$. The source was also used to obtain the relative gain calibration of the 13 MCPMT channels viewing the fibers of the 13 tiles of tower 1. It was found that the rms gain variation for these channels was $\pm 30\%$.

These 13 MCPMT channels were also calibrated with the LED and the same rms gain variation was observed as with the source. However, dividing the source output of each channel by the LED output resulted in an rms deviation of $\pm 8\%$, indicating agreement between the source and LED calibrations. Since it was not possible to illuminate the individual SMD strips with the source, the LED could not be calibrated against the source for the 16 MCPMT channels viewing the SMD. For the gain calibration of these channels we used the LED results.

4. Test-beam run and results

In a two-shift run on December 13-14 of 1991 we collected data for electrons at energies from 10 to 150 GeV and for muons at 175 GeV. The bulk of the data were taken with the beam roughly in the center of tower 3. These data are useful for evaluating energy linearity and resolution, as well as SMD position resolution and lateral electron shower profiles as a function of beam momentum. The second largest set of data was taken with the beam on tower 1, yielding the longitudinal electron shower profiles as a function of energy. A small amount of data with the beam on towers 2 and 4 serve for calibrating these towers in order to evaluate correctly the leakage from the showers of tower 3. Finally, the muon data are useful for establishing the muon to electron pulse height ratio to fix the calibration for future use.

Below we summarize our main results and comment on their significance. With the exception of the longitudinal electron shower profiles, which were obtained from tower 1, all results are from the data collected with the beam on tower 3. Energy resolutions are presented both for tower 1 and 3.

4.1 Linearity

The response of tower 3 to electrons of energies 30-150 GeV is shown in Fig. 6. The calorimeter is linear to better than 1% for energies above 50 GeV. At 30 GeV the response is down by about 1.7%. This small non-linearity is attributed to the coarse longitudinal segmentation of the calorimeter, which affects the lower energies as the shower maximum moves more and more forward with decreasing energy. The tendency for decreased response with decreasing energy is already detectable at the 50 GeV point, which is down by 0.8% relative to the points at higher energies.

4.2 Energy resolution

The energy resolution of the calorimeter is plotted in Fig. 7 as a function of $1/\sqrt{E}$. A linear fit to the data of tower 3 yields

$$\sigma(E)/E = A/\sqrt{E} + B$$

$$A = (22.5 \pm 0.5) \% \quad B = (0.21 \pm 0.05) \%$$

The A-term, which is mainly due to sampling fluctuations, is reasonable for a calorimeter of this granularity [2]. The constant term B is quite small, reflecting the small tile-to-tile variations within a tower.

The fit to the data of tower 1 yields $A = (25.8 \pm 0.5) \%$ and $B = (0.21 \pm 0.05) \%$. The A-term is about 15 % larger than that of tower 3. If this is attributed to the fact that the light from tower 1 is half as much, since it is collected only from one end of the WLS fibers rather than from both ends, one can calculate the contribution of sampling fluctuations to be 19%, and of photostatistics 13% for tower 3 and 18% ($13 \times \sqrt{2}$) for tower 1. From the photostatistics contribution of 13% for tower 3 one then deduces that there are 59 photoelectrons per GeV and hence $59 \text{ pe's/GeV} \times 1/13 \text{ layers} \times 1/(2.83 \text{ MIPs/GeV}) = 1.6 \text{ pe's/layer-MIP}$.

4.3 Position resolution

The radial position of the shower is determined from the energy distribution observed in the eight SMD strips. The relative calibration of the strips, including the gain of the MCPMT channels, was

obtained from LED measurements as mentioned above and from a position scan in which the beam was moved along the radius of the detector (perpendicular to the strips). Fig. 8 shows the correlation between the y-position obtained from the beam drift chambers and that calculated from the r-position determined by the SMD and a ϕ -angle of 67.5 degrees (the middle of tower 3). Fig. 9 shows the SMD position resolution as a function of energy. The resolution improves with increasing energy from the value of ± 2.1 mm at 30 GeV to ± 1.4 mm at 150 GeV. A fit to the form $A/\sqrt{E} + B$ yields $A = 6.5$ mm \cdot GeV $^{1/2}$ and $B = 0.83$ mm. The A-term is expected from sampling fluctuations while the constant term B is mostly due to the uncertainty in the beam position.

It should be emphasized that the resolution we obtained is much better than $(10.3 \text{ mm})/\sqrt{12} = 3$ mm, where 10.3 mm is the strip width of the SMD. This indicates that energy sharing among adjacent strips plays an important role. Since the shower full width is expected to be somewhat smaller than the SMD strip width [2,3], it seems that the optical communication (optical cross-talk) between strips in our SMD design (see section below for details) may actually be helpful in improving the position resolution.

4.4 Lateral shower profile

Lateral electron shower profiles obtained with the SMD are shown in Figs. 10 for 30 GeV and 150 GeV electrons. The two distributions are, as expected, very similar. A gaussian fit yields a width of ± 1.3 cm.

It is well known from data and simulations that electron showers consist of a narrow core with broad tails. The core has a full width of a few millimeters [3]. However, in a detector with wide strips the core is effectively "squashed down", resulting in a broader distribution. Optical cross-talk between strips, and electronic cross-talk among the MCPMT channels (small compared to the optical cross-talk in our case, as we will see below), tend to broaden this distribution even further. The optical cross-talk in the SMD was measured using electrons from a beta source. It was found that the response of the strip adjacent to the one through which the electron passed is about 30%, while that of the next strip over is about 8% (Fig. 11). Folding the results of these measurements with a GEANT Monte-Carlo electron shower simulation provides good fits to the shower profiles obtained in the test beam (Fig. 12).

Understanding and minimizing the optical cross talk between strips is crucial to the design of a SM detector that, in addition to good position resolution, is expected to provide good pi-zero/electron separation. However, since in the case of the microplugs we are interested in very high energy gamma showers (100 GeV or more), which would be difficult to separate from pi-zeros even with a detector with no cross-talk at all, we are content with a detector with just good position resolution. With this

goal in mind, optical cross talk, far from being harmful, may in fact contribute to better position resolution, as pointed out above. In order to obtain narrower shower profiles, one would have to reduce the level of optical cross-talk. This can be done by carving deeper separator grooves, or even by gluing the scintillator slab onto a sheet of aluminum and carving all the way down to the aluminum to eliminate cross-talk altogether.

4.5 Longitudinal shower profiles

The longitudinal shower profiles for electrons of 10, 100 and 150 GeV, obtained from data collected on tower 1, are presented in Fig. 13. The curves shown were calculated using the simple formulae of average shower behavior given in the particle properties data booklet. These curves are not actual fits to the data. However, as only one free parameter was used for normalizing all four curves to the corresponding data sets, the agreement with the data is satisfactory. The shifting of the shower maximum forward with decreasing energy is clearly observed as predicted.

4.6 Muons

A muon run at beam momentum of 175 GeV/c yielded the distribution shown in Fig. 14. The curve superimposed on the data is a Landau fit. By comparing the muon peak with our 100 GeV electron shower peak we obtain the ratio 2.83 ± 0.03 muons per GeV of electron shower energy.

5. Conclusion

Our results on linearity, energy resolution, longitudinal shower profiles and on muons are as expected for the type and granularity of EM calorimeter that we have built and tested. The performance of the shower maximum detector in measuring position is excellent. Given the simplicity of design and construction of this detector, we believe that its performance establishes it as a serious candidate for SMD's planned for large collider experiments. In the specific case of separator groove depth to scintillator thickness ratio that we have tested, optical cross talk broadens the shower lateral profile considerably. However, in experiments in which such broadening is undesirable, deeper grooves can be carved to reduce the optical cross talk, or even complete isolation between strips can be achieved by various techniques, as for example by gluing the scintillator slab on an aluminum sheet and carving all the way down to the metal. Regardless of how exactly it is implemented, this technique lends to simple, uniform and easy to construct shower maximum position detectors with excellent position resolution.

6. Acknowledgements

We wish to thank Vadim Sherman for his skillful machining of all detector elements, other than the lead and scintillator tiles that were manufactured by companies in Japan, and Eric Homes for making the initial measurements of the uniformity of light output from the tiles. We are indebted to the CDF collaboration for the use of their test beam facilities at Fermilab.

7. References

- [1] F. Abe et al., "The CDF Detector: An Overview", Nucl. Instr. and Meth. A271 (1988) 387-403.
- [2] P.B. Cushman, "Electromagnetic and Hadronic Calorimeters", Instrumentation in High Energy Physics, Vol.9 in "Advanced Series on Directions in High Energy Physics", Editor F. Sauli, World Scientific, Singapore (1992).
- [3] J. Hauser et al., "A Prototype Scintillating Fiber Position Detector for Electron and Photon Identification in High Luminosity Colliders", submitted to Nucl. Instr. and Methods.

Figure Captions

- Fig. 1 The Microplug calorimeter.
- Fig. 2 The shower-maximum position detector.
- Fig. 3 Aluminum cover of the position detector showing the way the fibers are inserted into the scintillator grooves.
- Fig. 4 Tower lay-out of the Microplug test module.
- Fig. 5 Schematic drawing of fiber arrangement in the Microplug test module
- Fig. 6 Linearity of tower 3: measured electron energy E over beam momentum p .
- Fig. 7 Electron energy resolution of towers 1 and 3.
- Fig. 8 Correlation of electron y -positions (vertical in Fig.4) measured with the beam drift chambers and with the shower-maximum position detector.
- Fig. 9 Position resolution obtained with the shower-maximum detector as a function of electron energy.
- Fig. 10 Lateral shower profiles for 30 GeV (solid line) and 150 GeV electrons obtained with the shower-maximum detector.
- Fig. 11 Light output as a function of detector strip with beta source on strip 4.
- Fig. 12 Comparison of lateral shower profile of 150 GeV electrons with Monte Carlo simulation.
Solid curve: GEANT Monte Carlo simulation.
Dashed curve: Monte Carlo folded with beta source measurements of optical cross-talk (see Fig. 11).
- Fig. 13 Longitudinal shower profiles for 10, 50 and 100 GeV electrons. The curves shown were calculated using the formulae of average shower behavior given in the particle data booklet and they are "eye-ball fits" to the data with one overall arbitrary constant.
- Fig. 14 Response of tower 3 to 175 GeV muons. The curve is a Landau fit to the data.

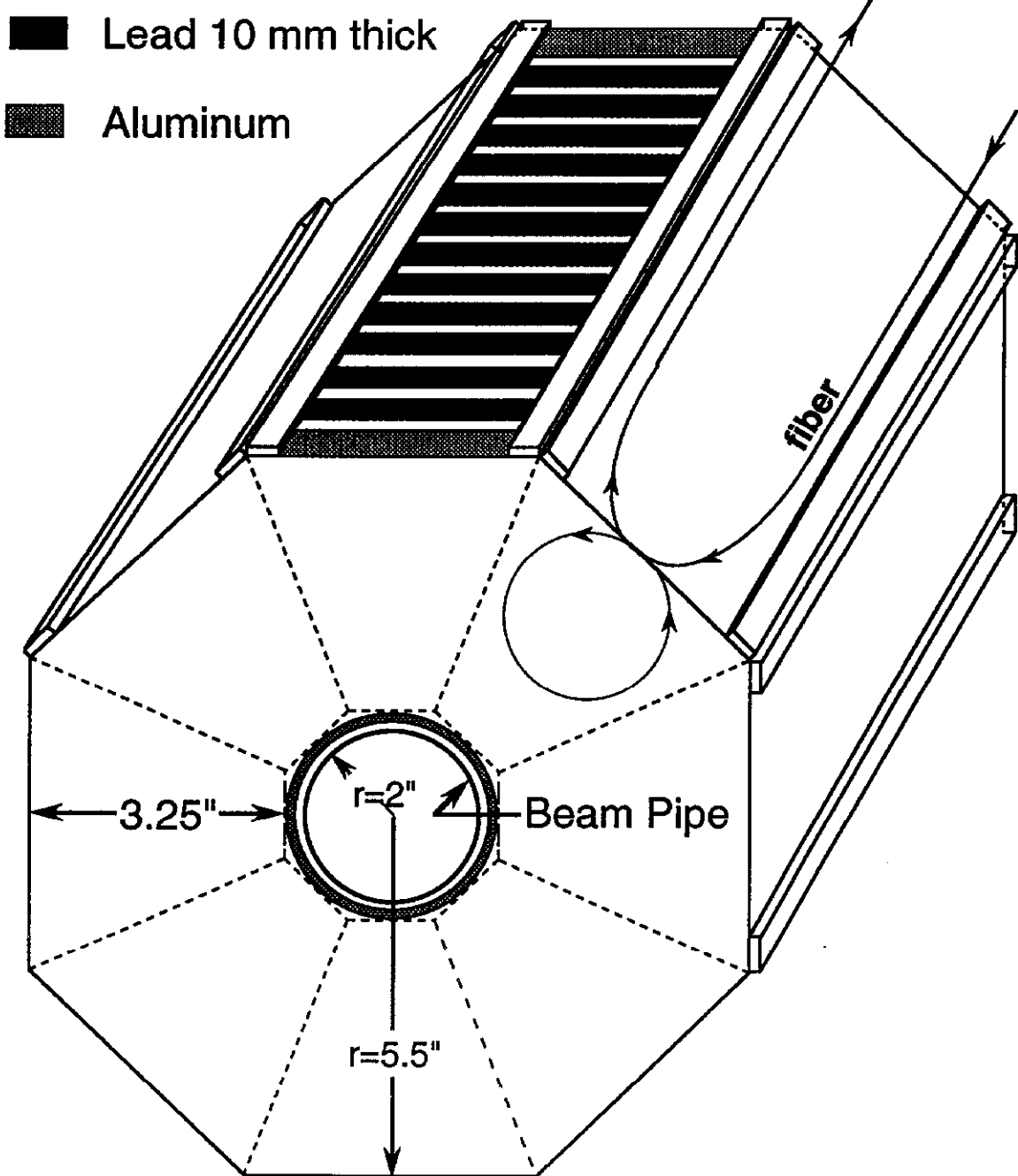


Figure 1

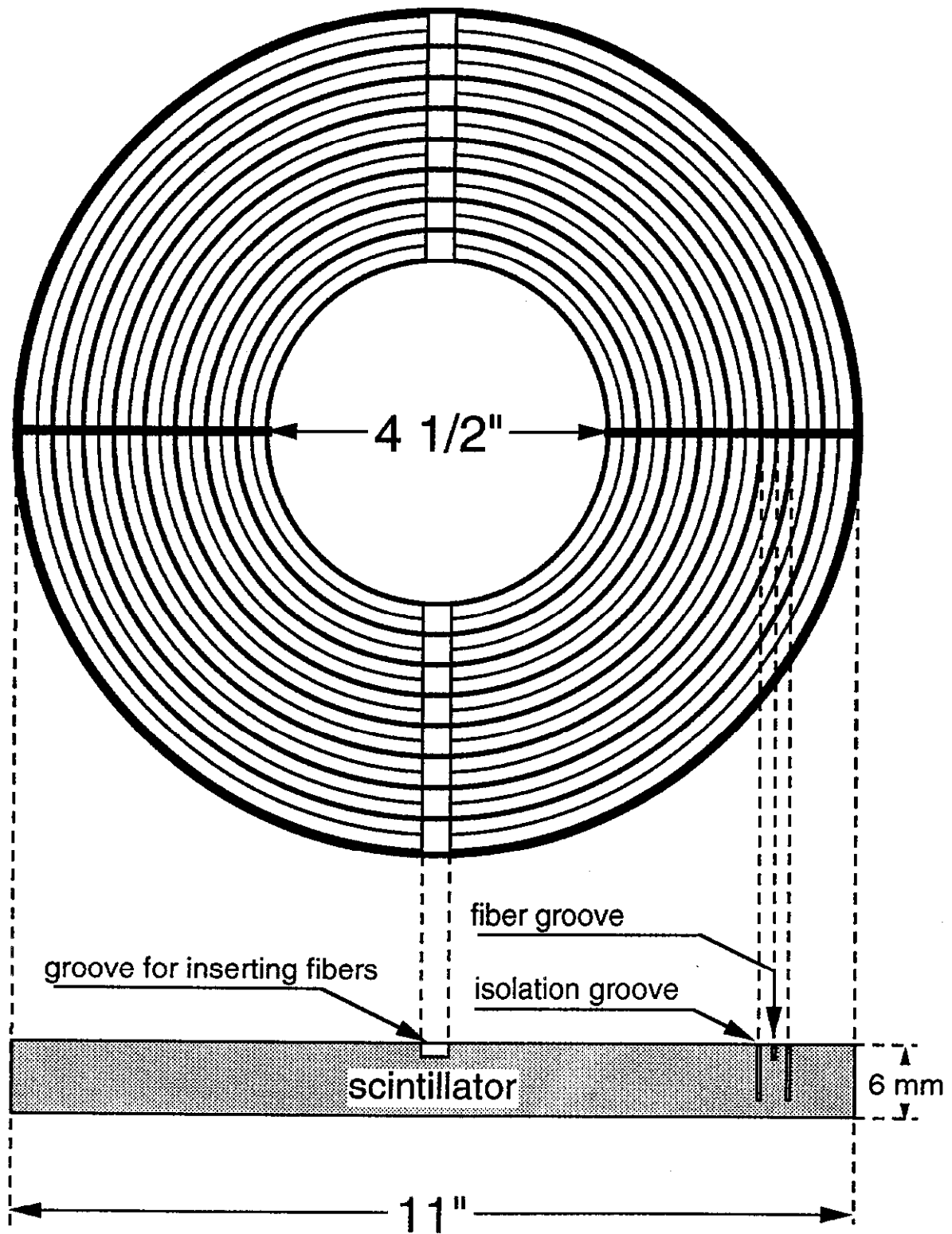


Figure 2

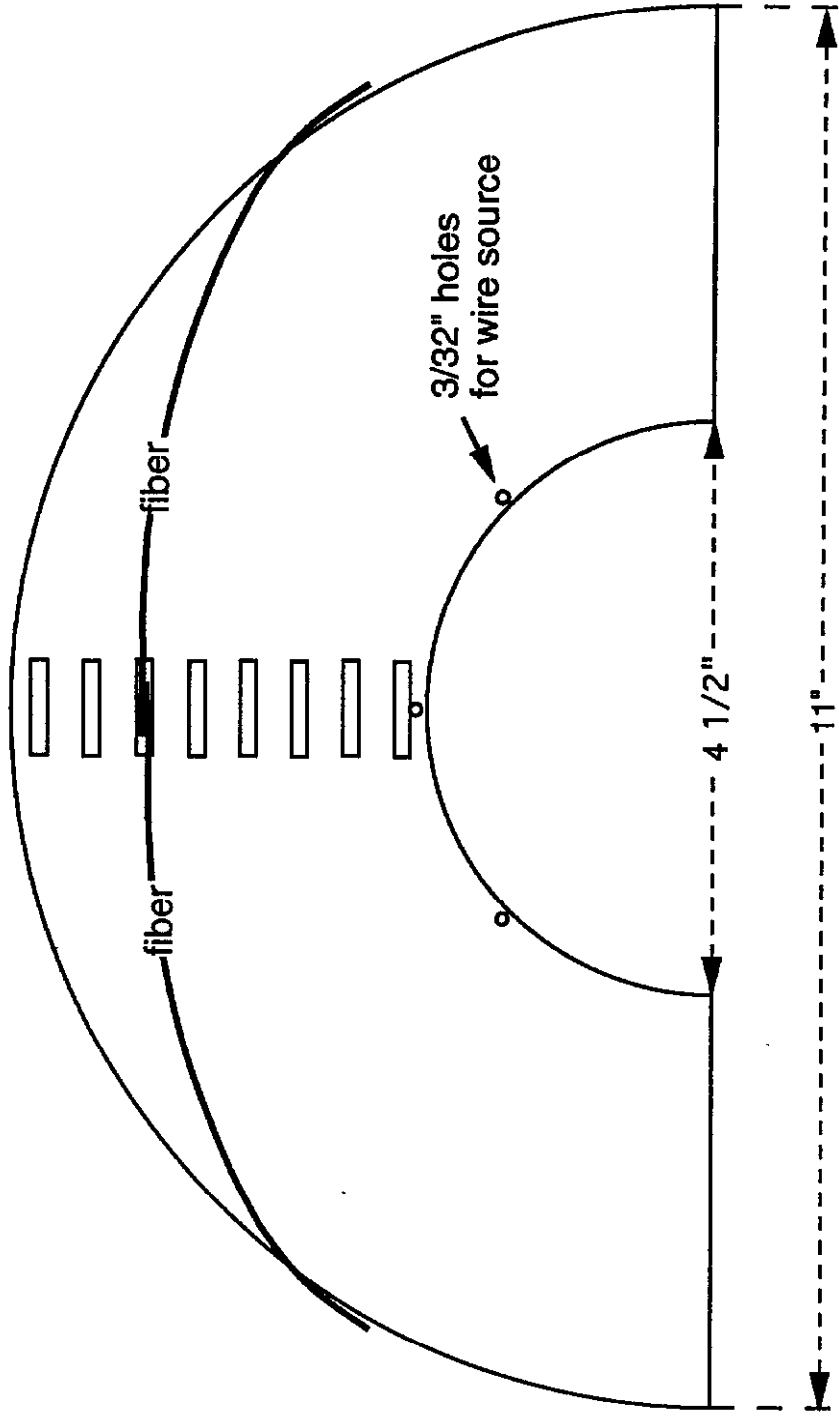


Figure 3

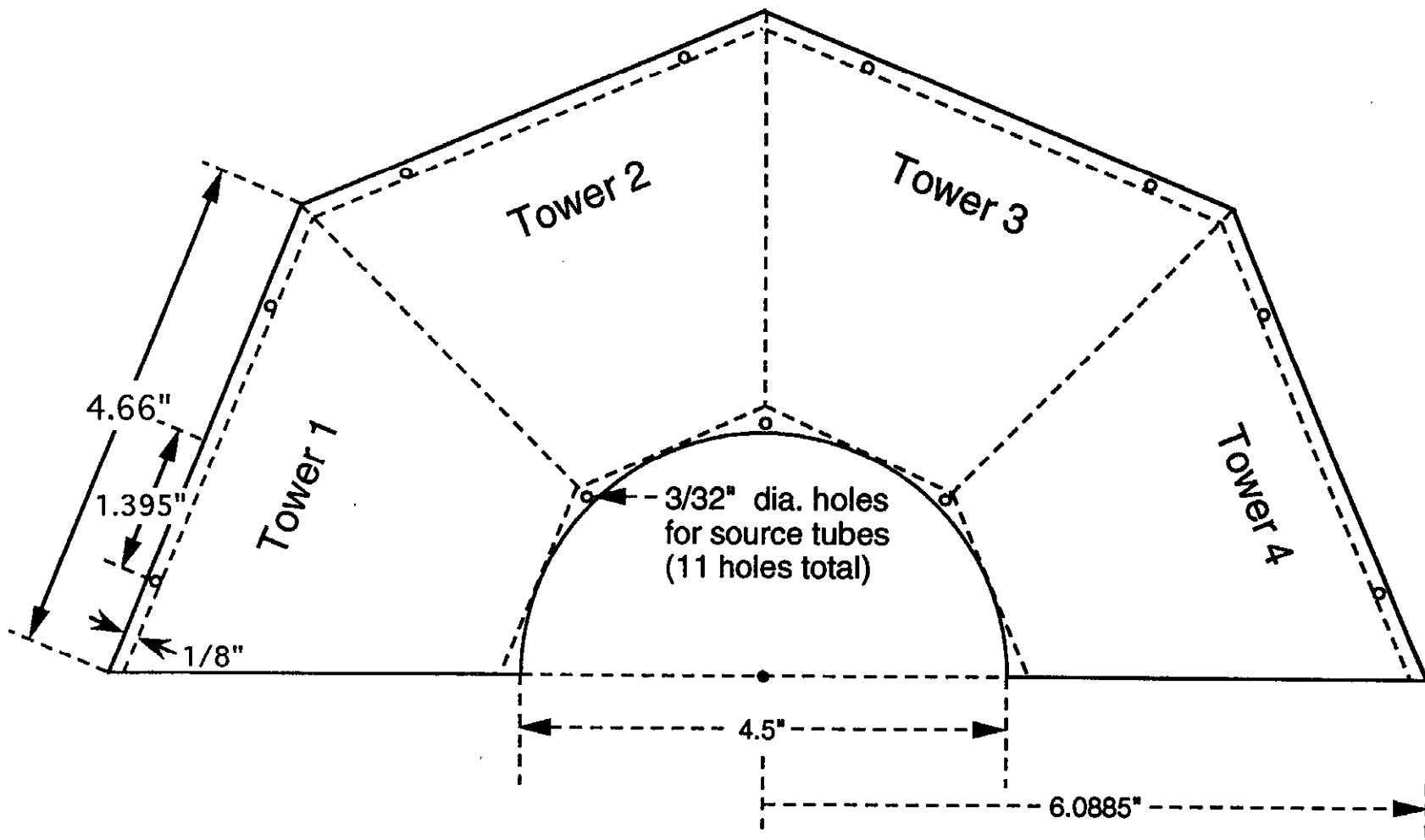


Figure 4

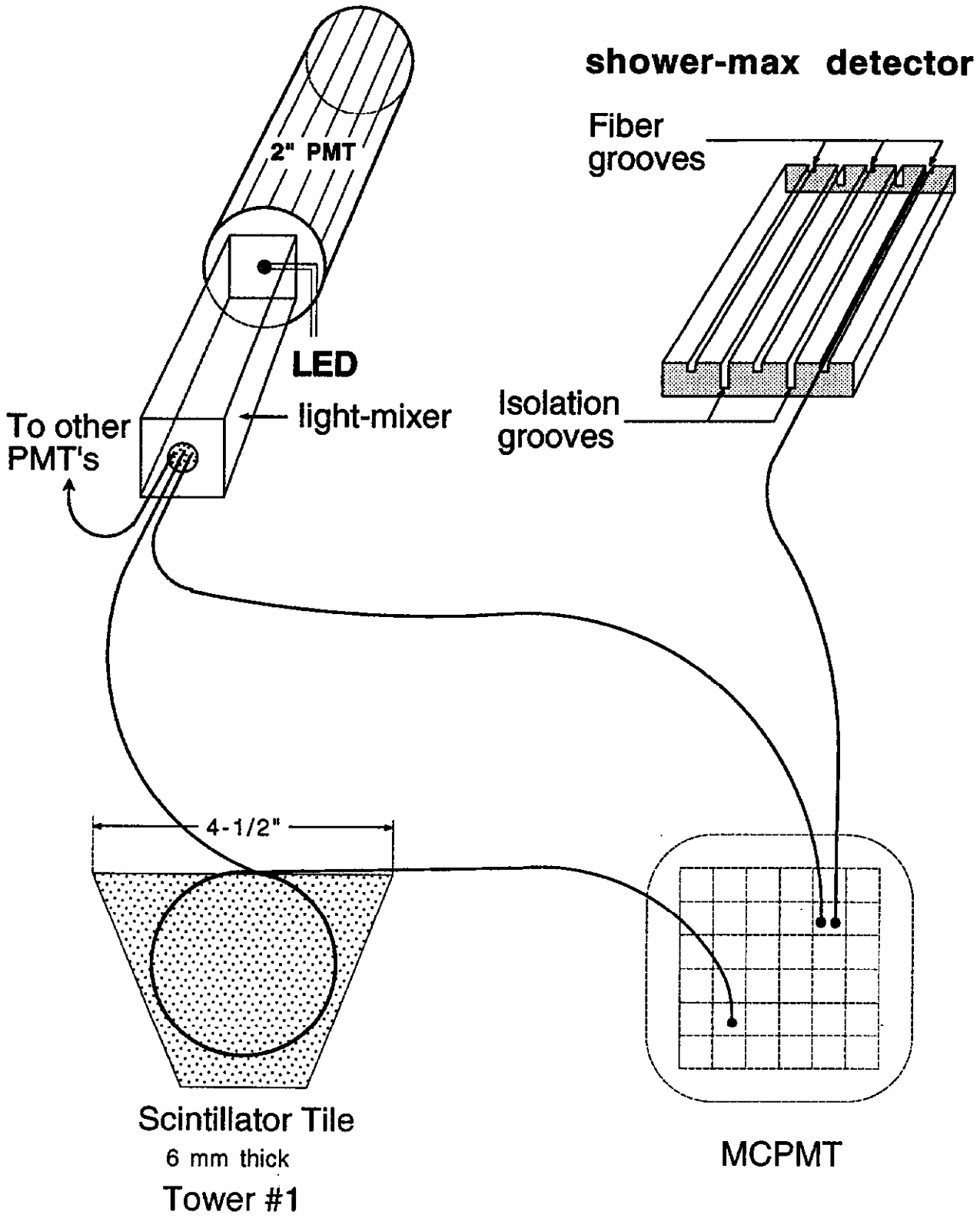


Figure 5

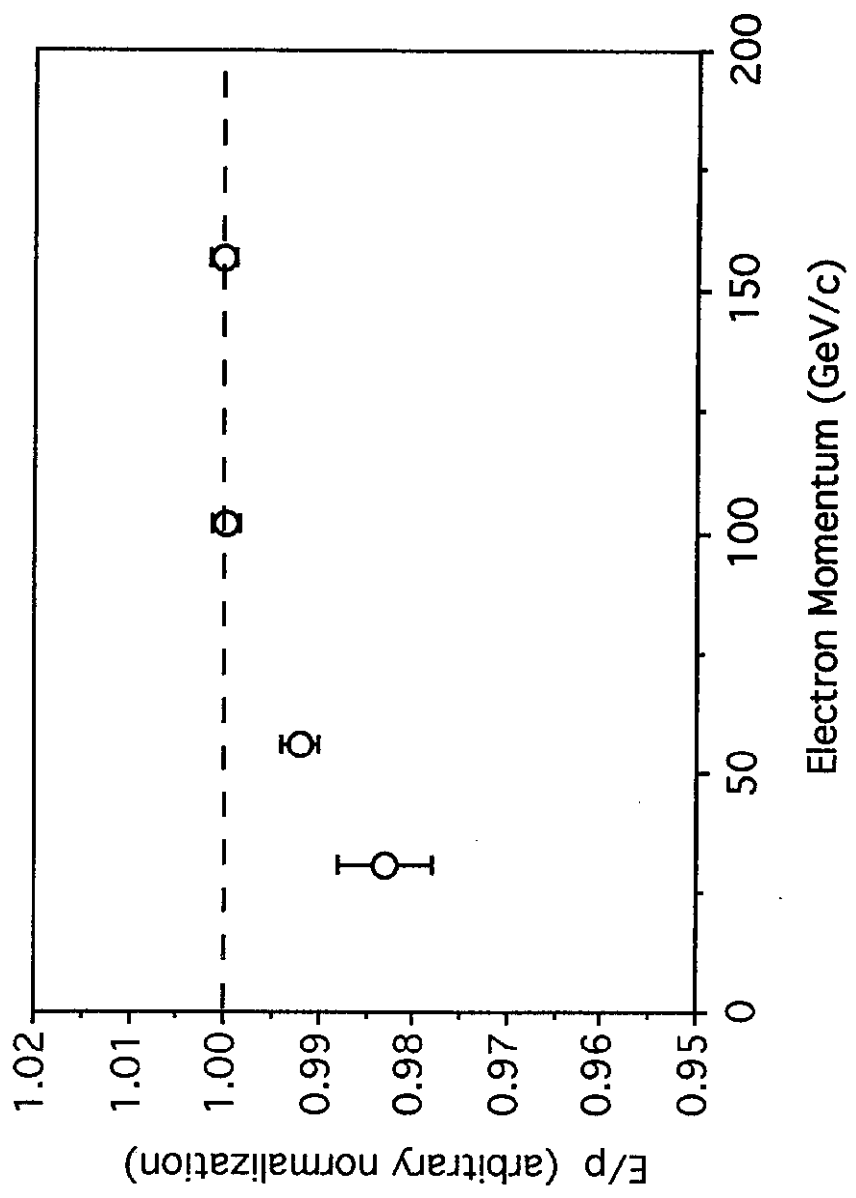


Figure 6

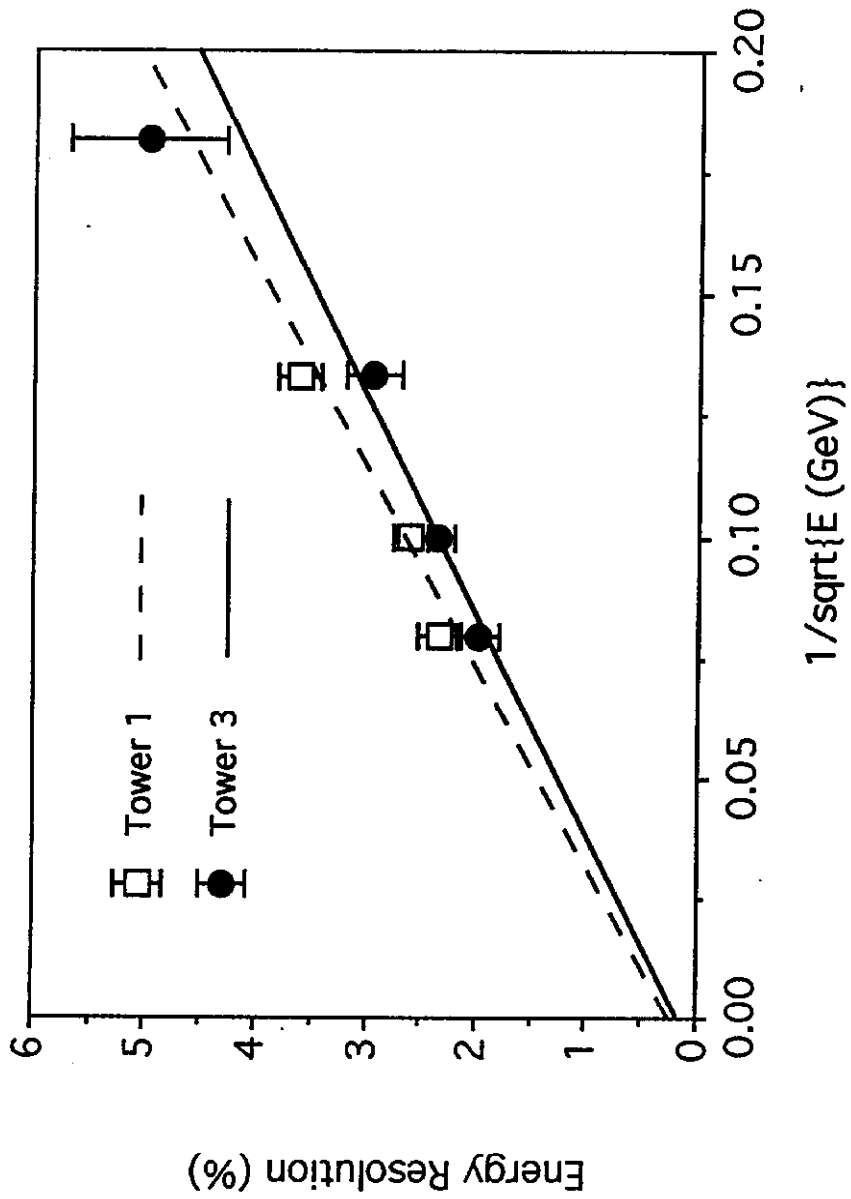


Figure 7

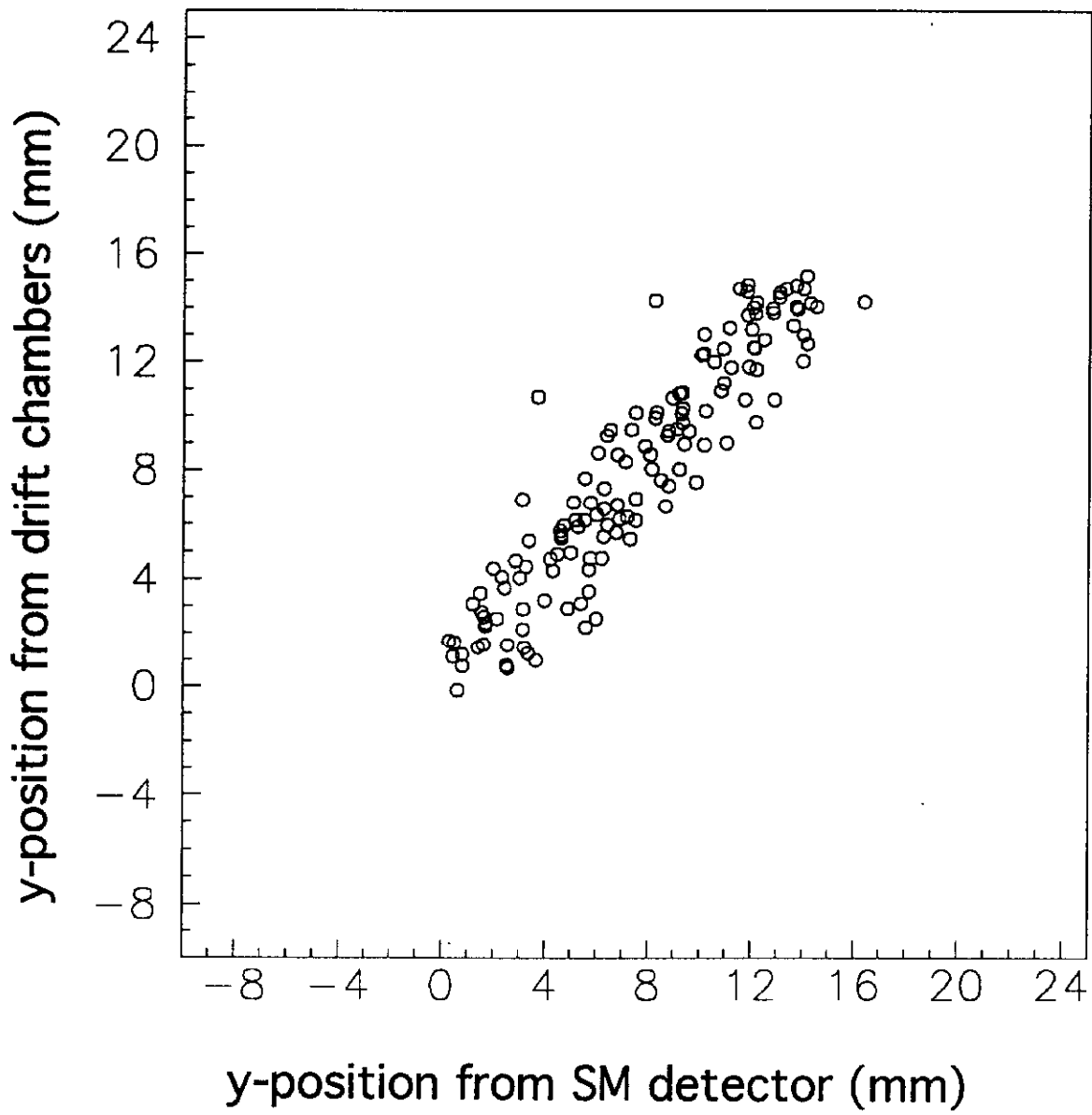


Figure 8

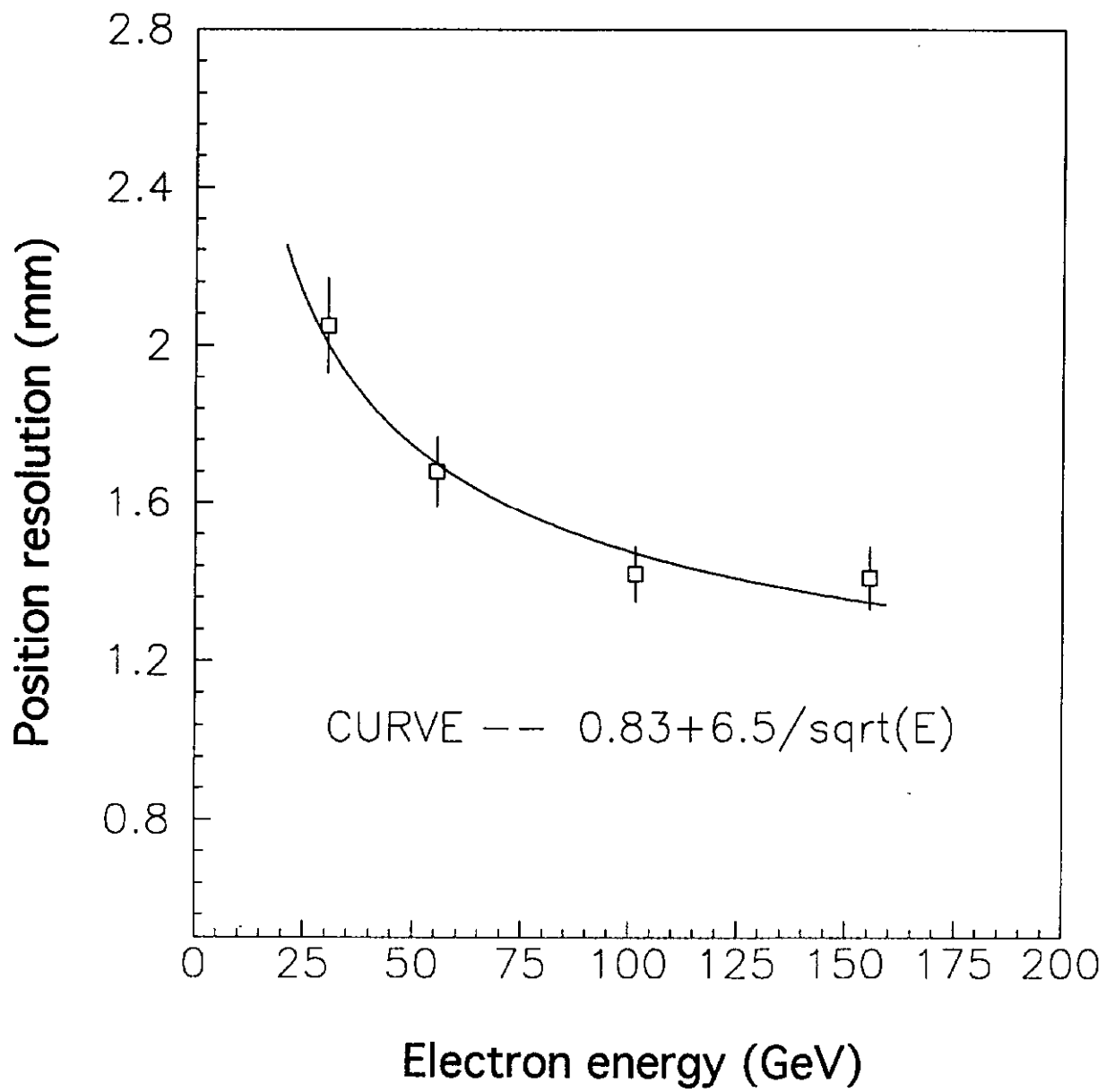


Figure 9

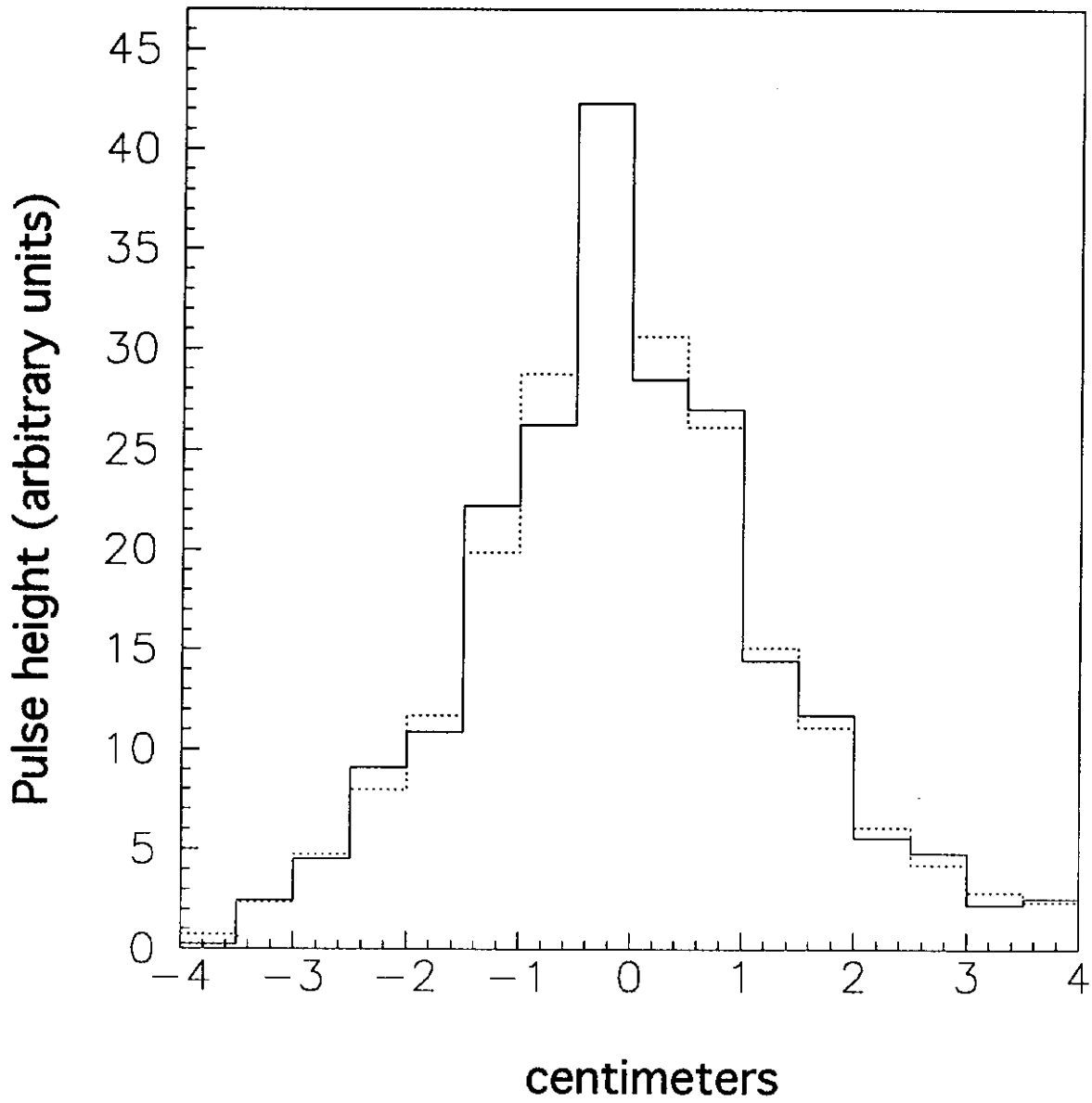


Figure 10

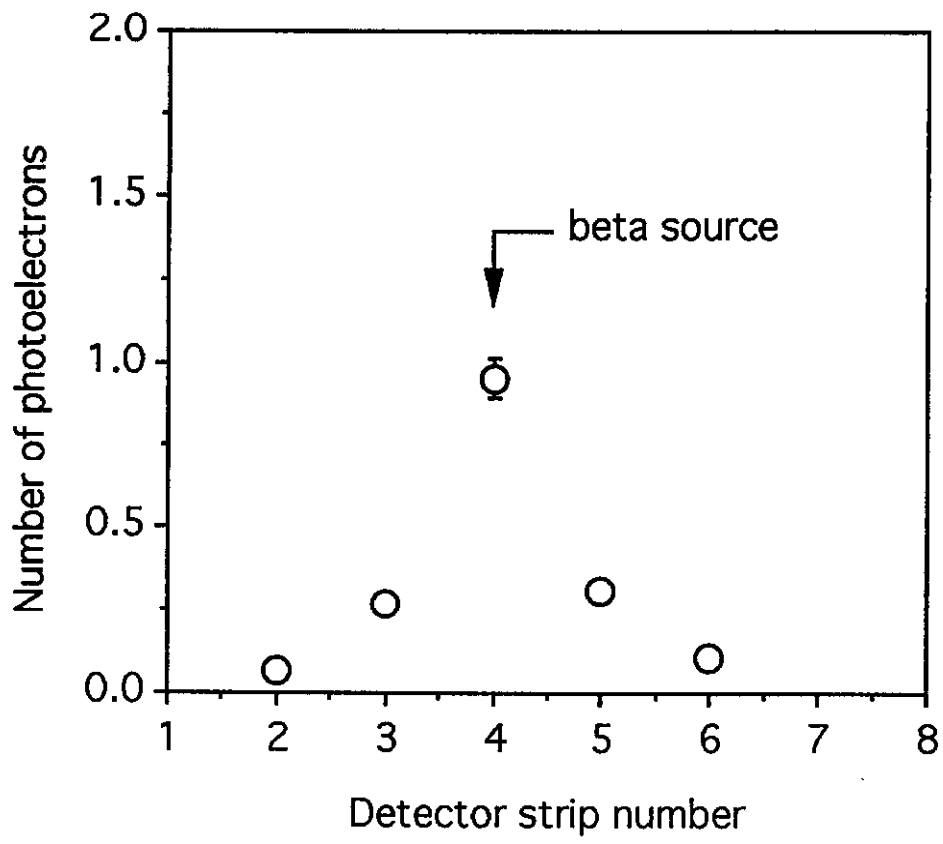


Figure 11

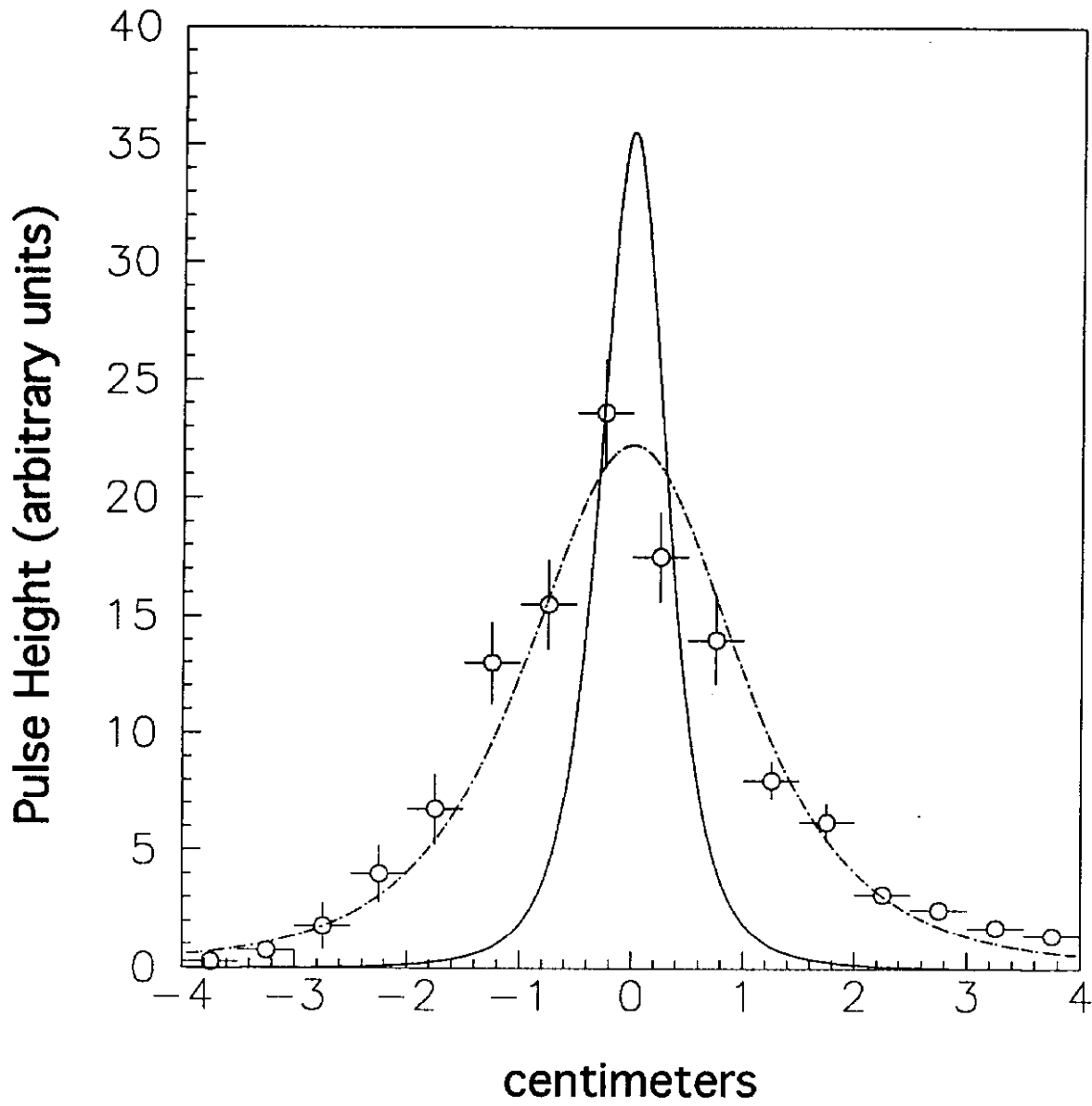


Figure 12

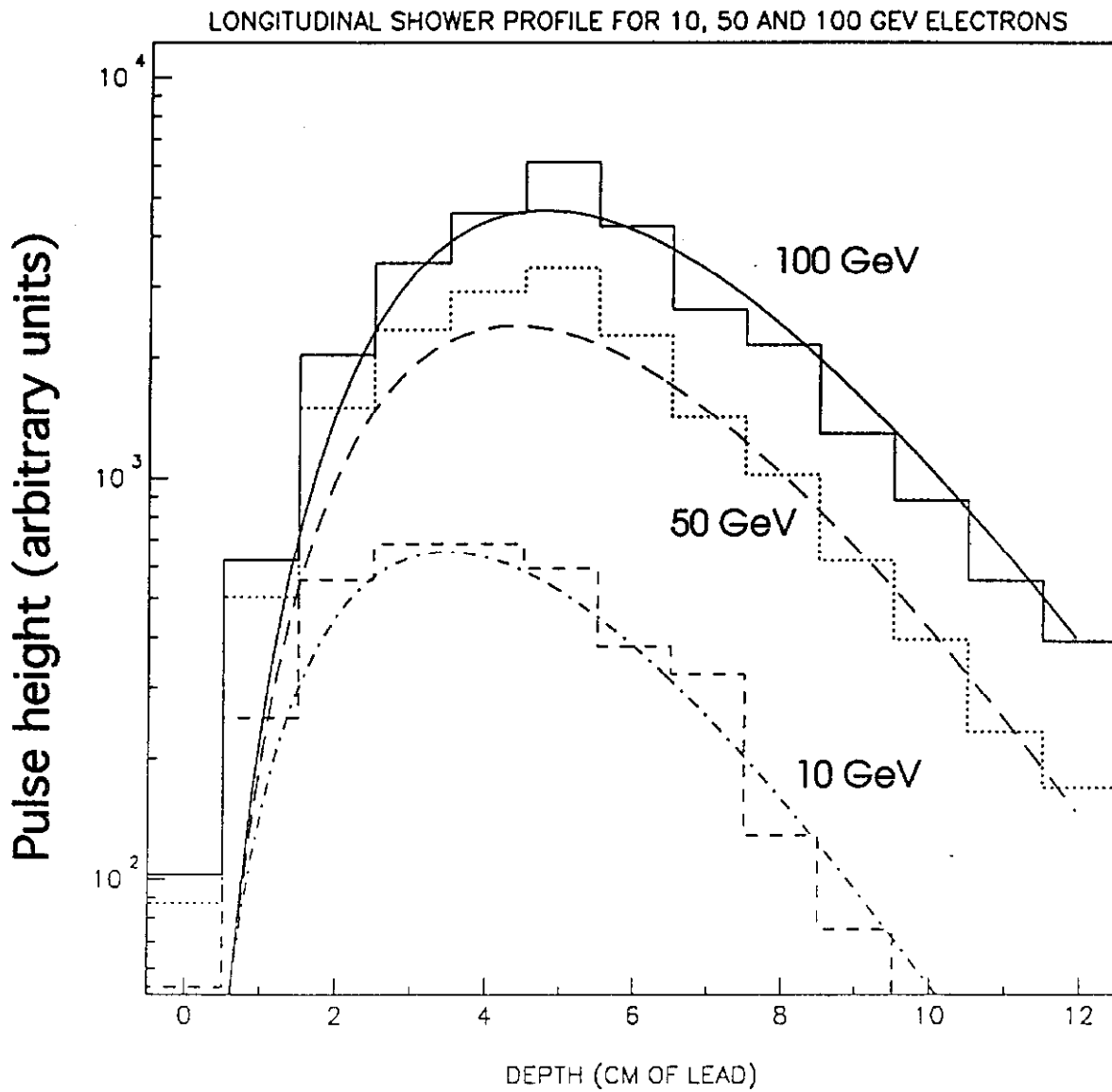


Figure 13

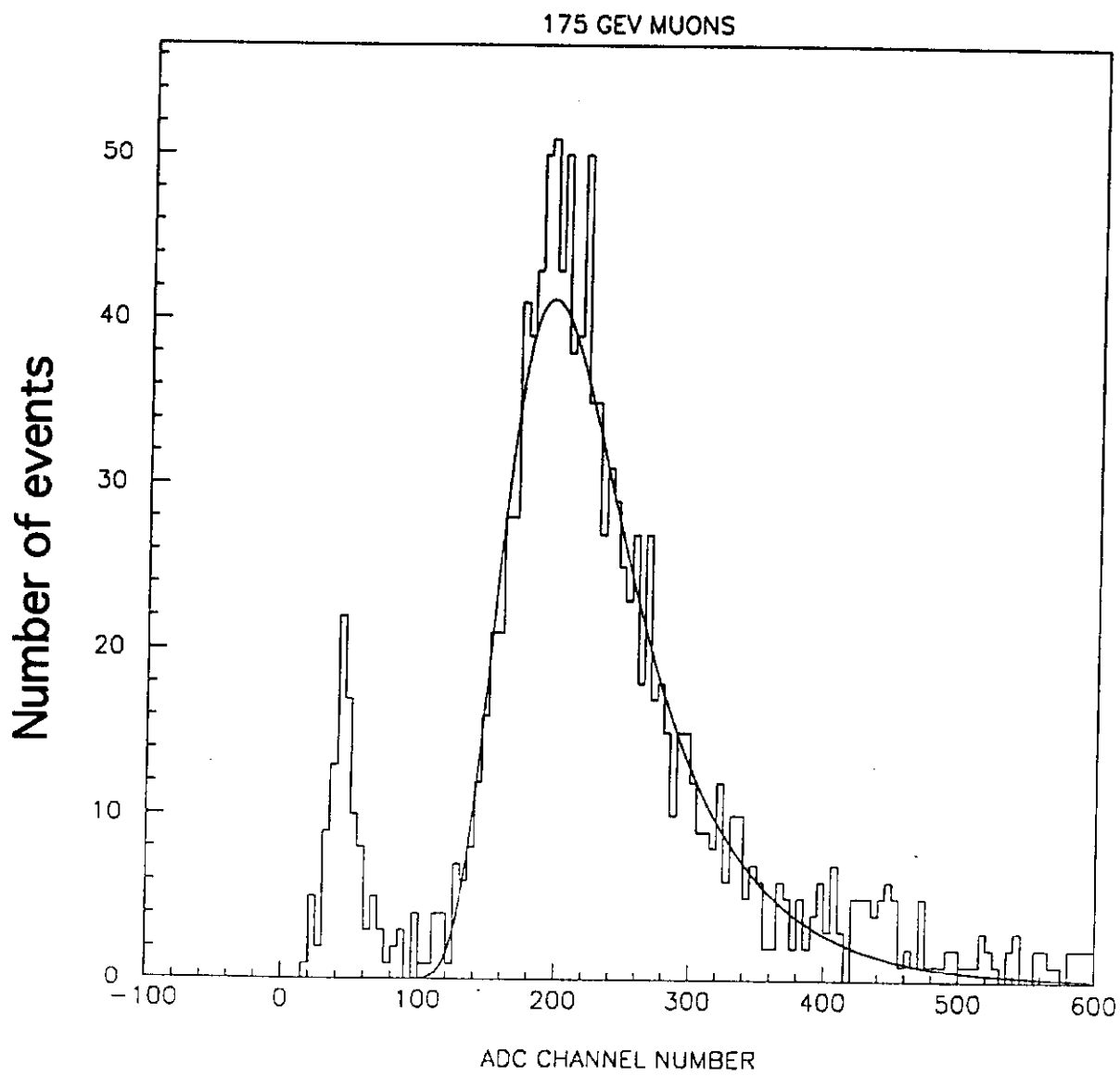


Figure 14